Metal Ion Activation of *S*-Adenosylmethionine Decarboxylase Reflects Cation Charge Density†

Zichun J. Lu and George D. Markham*

Institute for Cancer Research, Fox Chase Cancer Center, 333 Cottman Avenue, Philadelphia, Pennsylvania 19111

Received December 19, 2006; Revised Manuscript Received April 3, 2007

ABSTRACT: *S*-Adenosylmethionine decarboxylase from *Escherichia coli* is a pyruvoyl cofactor-containing enzyme that requires a metal cation for activity. We have found that the enzyme is activated by cations of varying charge and ionic radius, such as Li^{+}, $A1^{3+}$, Tb^{3+}, and Eu^{3+}, as well as the divalent cations Mg^{2+}, Mn^{2+}, and Ca^{2+}. All of the activating cations provide k_{cat} values within 30-fold of one another, showing that the charge of the cation does not greatly influence the rate-limiting step for decarboxylase turnover. Cation concentrations for half-maximal activation decrease by >100-fold with each increment of increase in the cation charge, ranging from ∼300 mM with Li^{+} to ∼2 μM with trivalent lanthanide ions. The cation affinity is related to the charge/radius ratio of the ion for those ions with exchangeable first coordination sphere ligands. The exchange-inert cation $Co(NH_3)_6^{3+}$ activates in the presence of excess EDTA (and NH_4^{+} does not activate), indicating that direct metal coordination to the protein or substrate is not required for activation. The binding of metal ions (monitored by changes in the protein tryptophan fluorescence) and enzyme activation are both cooperative with Hill coefficients as large as 4, the active site stoichiometry of this $(\alpha\beta)_4$ enzyme. The Hill coefficients for Mg^{2+} binding and activation increase from 1 to ∼4 as the KCl concentration increases, which is also observed with NaCl or KNO_3; neither Na^{+} nor K^{+} activates the enzyme. The single tryptophan in the protein is located 16 residues from the carboxyl terminus of the pyruvoyl-containing α chain, in a 70-residue segment that is not present in metal ion independent AdoMet decarboxylases from other organisms. The results are consistent with allosteric metal ion activation of the enzyme, congruent with the role of the putrescine activator of the mammalian AdoMet decarboxylase.

Approximately one-third of all enzyme-catalyzed reactions are estimated to require a metal ion or ions (*1*), which is likely an underestimation when the oft-overlooked monovalent cation activation is considered (*2*−*4*). The functions of these metal ions can be considered as comprising several broad categories: (1) protein structural integrity (i.e., no specific role in catalysis), (2) electrophilic catalysis, (3) electron transfer reactions, and (4) allosteric regulation. In the first two instances a variety of metal ions of similar charges and sizes can often be used, albeit with varying potency. Understanding the relationships between the structures of proteins and their ability to discriminate among metal ions continues to be an important aspect of bioinorganic chemistry (*5*).

S-Adenosylmethionine decarboxylase (AdoMetDC)[1] from *Escherichia coli* is one of these metal ion dependent enzymes. AdoMetDC catalyzes the reaction that commits the multifunctional *S*-adenosylmethionine (AdoMet) to participation in polyamine biosynthesis (*6*−*8*). AdoMetDC is widely distributed in nature, having been described in eucarya, prokarya, and archaea (*9*−*12*). All known AdoMetDCs are encoded by a gene which directs synthesis of a precursor protein (π) that self-cleaves to yield a pyruvoyl cofactor containing subunit (α) and a second subunit (β) that arises from the N-terminal segment of the precursor polypeptide (*13*). Similar to the mechanisms of many other amino acid decarboxylases, in the AdoMetDC reaction a Schiff base intermediate forms between the substrate and a protein-bound cofactor, activating the α-carbon for nonoxidative decarboxylation (*12*, *14*, *15*). During the AdoMetDC reaction the pyruvoyl group forms a Schiff base with the substrate, which relieves the enzyme from a requirement for a pyridoxal cofactor as an electrophilic catalytic moiety (*12*); model studies indicate that pyruvoyl and pyridoxal cofactors have comparable catalytic potency (*16*).

AdoMetDC proteins comprise three distinct classes with widely differing sizes and sequences; there is <20% sequence identity between members of the different classes. Eucaryotic AdoMetDC are clearly homologous in sequence and structure (*15*). Many eucaryotic AdoMetDC are activated by the polyamine putrescine, which is a substrate for the next metabolic reaction, spermidine synthesis; spermidine synthesis and the subsequent spermine synthesis are the sole

† This work was supported by National Institutes of Health Grants GM31186 and CA06927 and also supported by an appropriation from the Commonwealth of Pennsylvania. The contents of this manuscript are solely the responsibility of the authors and do not necessarily represent the official views of the National Cancer Institute or any other sponsoring organization.

* To whom correspondence should be addressed. Telephone: (215) 728-2439. Fax: (215) 728-3574. E-mail: gd_markham@fccc.edu.

[1] Abbreviations: AdoMet, *S*-adenosyl-L-methionine; AdoMetDC, *S*-adenosyl-L-methionine decarboxylase; dcAdoMet, decarboxylated *S*-adenosylmethionine (i.e., *S*-adenosyl-3-methylthiopropylamine); MGBG, methylglyoxal bis(guanylhydrazone); CD, circular dichroism.

10.1021/bi6025962 CCC: $37.00
Published on Web 06/13/2007

consumers of decarboxylated AdoMet. A second, less studied, class of AdoMetDC, which is found in Gram-negative bacteria, requires a metal ion, presumably Mg^{2+} in vivo, for activity; the *E. coli* enzyme is the prototype of this class (*17*, *18*). The third class comprises metal-free, activator-independent enzymes with α and β subunits of <70 amino acids each, totaling approximately one-half the size of the eucaryotic AdoMetDC (αβ) unit. The third class was initially identified in the Gram-positive bacterium *Bacillus subtilis* (*10*) and the archaeon *Methanococcus jannaschii* (*9*); sequence analyses indicate that this class occurs throughout archaea and in diverse bacteria. Crystal structures have been reported for the eucaryotic class 1 putrescine-activated $(\alpha\beta)_2$ human enzyme (*19*) and the homologous activator-independent (αβ) potato enzyme (*20*) as well as the class 3 $(\alpha\beta)_2$ *Thermotoga maritima* enzyme (*21*). Crystallographic studies demonstrated that each (αβ) unit of the *T. maritima* AdoMetDC is topologically equivalent to one-half of the eucaryotic (αβ) unit (*21*), suggesting a gene duplication followed by functional divergence in eucarya (*9*). No protein structural information is available for a member of the metal ion requiring group.

AdoMetDC from *E. coli* has an $(\alpha\beta)_4$ composition with 17.7 and 12.4 kDa α and β chains, respectively. This AdoMetDC requires a metal cation such as Mg^{2+} for activity and is not activated by putrescine (*13*, *17*, *18*, *22*). Mn^{2+} binding studies showed a stoichiometry of one cation site per pyruvoyl group (*17*). Amino acid decarboxylases typically use either a metal ion activator or a Schiff base mechanism (*12*, *23*); thus *E. coli* AdoMet decarboxylase is unusual in utilizing both activators. We have investigated the selectivity of the *E. coli* protein for various metal ions in order to unmask the specificity of the cation in catalysis. The enzyme possesses a remarkable promiscuity for metal ions which allows activation by specific ions with charge ranging from +1, to +3 and even utilizes a cation with an exchange-inert first coordination sphere.

EXPERIMENTAL PROCEDURES

Reagents were obtained from Sigma unless otherwise noted. Metal ion salts were purchased from Alfa Inorganics. $CrCl_3$ was converted to the aquo cation by heating of an aqueous solution until the changes in the visible spectrum were complete. Methylglyoxal bis(guanylhydrazone) (MGBG) is a general inhibitor of AdoMetDCs, and immobilized MGBG has been used to purify these enzymes from various sources (*9*, *17*, *24*). An affinity resin of MGBG-Sepharose was prepared by reacting 0.2 M MGBG with epoxy-activated Sepharose 6B (GE Pharmacia) for 18 h at pH 9, followed by extensive washing with 1 M KCl and then with water before use (*17*).

AdoMetDC Purification. The plasmid containing the structural gene for *E. coli* AdoMetDC (*speD*) was obtained from Drs. C. W. and H. Tabor, National Institutes of Health (*25*) and is referred to herein as pECDC. The plasmid was transformed into strain BL21(DE3)-(codon-plus-RIL) (Stratagene) for protein expression. A small culture (typically 10 mL) of the resultant BL21(DE3)-(codon-plus-RIL)pECDC was grown overnight at 37 °C in LB medium containing 50 μg/mL carbenicillin. Larger volumes of LB media were then inoculated with a 1:20 dilution (v/v) of the overnight culture and grown at 37 °C for 4 h. AdoMetDC expression was then induced by the addition of 0.1 mM isopropyl 1-thio-(β-D-galactopyranoside), followed by growth for an additional 3 h. Cells were harvested by centrifugation and stored at −80 °C until use.

All purification steps were conducted at room temperature. In a typical preparation, 25 g (wet weight) of cells, obtained from 6 L growth, was suspended in 250 mL of 50 mM Tris·HCl, 50 mM KCl, and 30 μM phenylmethanesulfonyl fluoride (pH 8). The cells were lysed by a single pass through a French press at 15000 psi. The lysate was centrifuged for 30 min at 25000*g* to remove insoluble material.

Solid KCl was added to the supernatant solution to a final concentration of 0.6 M; 1 M $MgCl_2$ was added to a final concentration of 10 mM, and the pH of the extract was adjusted to 8.0 with 5 N KOH. The solution was then loaded onto a column (2 × 20 cm) of MGBG-Sepharose which had been equilibrated with 20 mM Tris·HCl, 10 mM $MgCl_2$, and 0.6 M KCl, pH 8. After loading, the column was washed with the same buffer until the absorbance at 280 nm of the eluate was the same as that of the buffer. AdoMetDC was then eluted by washing the column with 20 mM potassium phosphate, 0.8 M KCl, and 0.5 mM EDTA, pH 7. Trace impurities were removed by ion-exchange chromatography as previously described, except that a Q-Sepharose matrix was used in place of DEAE-Sephadex (*17*).

Protein purity was verified by polyacrylamide gel electrophoresis on 8−25% gradient gels using a Pharmacia (GE) PhastSystem. A single band was observed upon native electrophoresis, and the expected two bands were observed upon SDS denaturing electrophoresis (*26*).

Enzyme concentrations were determined from the absorbance at 280 nm using an extinction coefficient of 0.84 $(mg/mL)^{-1}\ cm^{-1}$, calculated by the method of Mach et al. (*27*). A monomeric molecular mass of 30.1 kDa for the (αβ) heterodimer was used for calculation of molar concentrations (*13*).

Kinetic Analyses of AdoMetDC Activity. AdoMetDC activity was assayed by measuring the production of $^{14}CO_2$ from [*carboxy*-^{14}C]AdoMet (Moravek). Routine reaction mixtures (100 μL) contained 0.2 mM AdoMet, 50 mM Hepes·KOH, pH 7.5, 10 mM $MgCl_2$, and 50 mM KCl. The vials were sealed with filters soaked with 50 μL of a saturated solution of $Ba(OH)_2$ in the caps. Reactions were stopped after 1−10 min by the addition of 100 μL of 4 N HCl. After the samples were shaken for 30 min at room temperature, the $^{14}CO_2$ absorbed on the filters was quantified by scintillation counting (*18*). Kinetic analyses of AdoMetDC activity with other metal ions also measured the production of $^{14}CO_2$ from [*carboxy*-^{14}C]AdoMet; protein concentrations were adjusted so that $^{14}CO_2$ formation was linear with time (*28*). Determination of the pH variation in V_{max} was conducted in the presence of 10 mM $MgCl_2$ or 10 μM $TbCl_3$, as described previously (*28*). Kinetic data were fit to the Michaelis−Menten or Hill equations. Fluorescence binding data were fit to analogous equations plus an offset for the nonzero fluorescence in the absence of ligands. The SigmaPlot Program (SPSS Inc.) was used for fitting.

Spectroscopic Measurements. Fluorescence studies monitored changes in intrinsic protein fluorescence. Either a Perkin-Elmer LS-50 luminescence spectrophotometer or a Cary Eclipse fluorescence spectrophotometer was used.

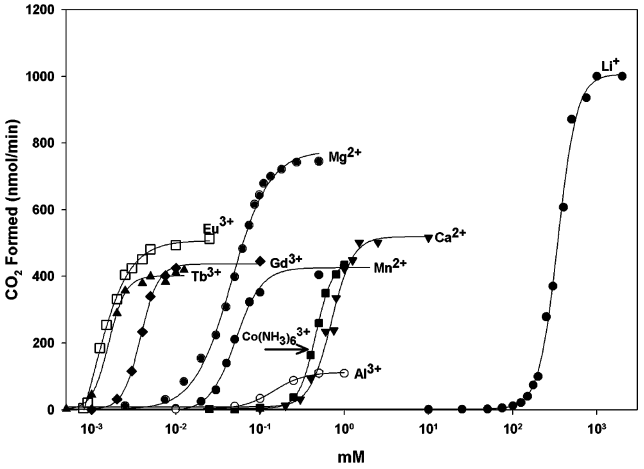

FIGURE 1: Activation of AdoMetDC by various metal ions. Solutions contained 50 mM Hepes·KOH and 50 mM KCl, pH 7.5 at 25 °C. The AdoMet concentration was 0.2 mM, except for $AlCl_3$ and LiCl where 0.8 mM AdoMet was used; the majority of these data are not at a saturating AdoMet concentration. Lines are fits to the Hill equation.

Unless stated otherwise, the excitation wavelength was 280 nm (bandwidth = 5 nm), and the fluorescence emission at 342 or 350 nm (bandwidth = 5 nm) was monitored. Solutions (2 mL) contained 1−2 μM $\alpha\beta$ protein in 10 mM Tris·HCl, pH 7.5. Experiments were performed at 25 °C, and the data were corrected for buffer contributions.

Circular dichroism spectra were recorded on an Aviv Model 62A spectropolarimeter. Samples (10 μM protein in 10 mM Tris·HCl, pH 7.5) were placed in 1 mm path length cells; spectra were recorded from 200 to 260 nm and were corrected for buffer contributions. A DynaPro dynamic light scattering instrument (Protein Solutions Inc.) was used to monitor the hydrodynamic radius of the enzyme. Protein (~1 mg/mL) in 25 mM Tris·HCl, pH 7.5, buffer at 25 °C was filtered through a 0.2 μm membrane into a light scattering cuvette. The hydrodynamic radius was determined in buffer alone and in the presence of either 10 mM $MgCl_2$ or 50 mM KCl or the combination of 10 mM $MgCl_2$ and 50 mM KCl.

RESULTS

Kinetic Studies of Metal Ion Activation. In the limited reported studies, the activation of *E. coli* AdoMetDC by metal ions was described as restricted to divalent cations that are typically considered as "hard" (Mg^{2+}, Mn^{2+}, Ca^{2+}), with no activity being observed in the presence of "soft" ions such as Cu^{2+} or Cd^{2+} or the monovalent cations Na^+ or K^+ (*17*, *18*). In the present studies, a wide variety of cations were investigated both for binding and for activation.

Figure 1 illustrates representative data for the activation by selected cations. Kinetic parameters obtained at saturating AdoMet and optimal metal ion concentrations are listed in Table 1. Because significant ionic strength changes occurred in some experiments, the effects of monovalent salts on the activity of the Mg^{2+}-activated enzyme were examined. Surprisingly, the activation by Mg^{2+} became positively cooperative in the presence of salt, with the Hill coefficient increasing from 1 to 3.4 (Figure 2A). KCl, NaCl, and KNO_3 acted equivalently, with a half-maximal effect at 110 mM salt (data not shown). The maximal reaction rate did not vary with the KCl concentration. The concentration of $MgCl_2$ required for half-maximal activation increased with the KCl concentration, indicating that higher ionic strength diminished the affinity of Mg^{2+}. To attenuate this salt effect, 50 mM KCl was included in experiments unless noted. The dependence of activity on AdoMet concentration did not vary with KCl concentration and remained noncooperative in all cases.

Table 1: Activation of *E. coli* AdoMet Decarboxylase by Different Metal Ions[a]

activator	n	K_a, μM	K_m(AdoMet), μM	V_{max} [nmol/(min·mg)]
Li^+ [b]	4.0 ± 0.3	(331 ± 8) × 10^3	219 ± 57	995 ± 24
Mg^{2+}	2.0 ± 0.1	79 ± 10	106 ± 28	932 ± 31
Ca^{2+}	3.0 ± 0.5	731 ± 64	117 ± 13	721 ± 42
Mn^{2+}	3.0 ± 0.3	51 ± 3	45 ± 17	422 ± 17
Fe^{2+}	3.7 ± 0.3	90 ± 9	121 ± 20	754 ± 65
Fe^{3+}	2.7 ± 0.5	134 ± 11	194 ± 24	34 ± 2
Co^{2+}	2.2 ± 0.2	38 ± 1	286 ± 53	274 ± 36
$Co^{3+}(NH_3)_6$ [b]	4.2 ± 0.2	457 ± 5	173 ± 23	573 ± 46
Al^{3+}	2.3 ± 0.2	143 ± 6	850 ± 43	316 ± 138
Tb^{3+}	4.2 ± 0.4	1.6 ± 0.6	151 ± 39	579 ± 85
Gd^{3+}	4.1 ± 0.3	3.8 ± 0.1	43 ± 17	430 ± 70
Eu^{3+}	3.5 ± 0.3	1.5 ± 0.1	95 ± 19	697 ± 67

[a] n is the Hill coefficient for the concentration dependence of metal ion activation, K_a is the concentration for half-maximal activation, K_m is the Michaelis constant for AdoMet, and V_{max} is the maximal velocity at saturating metal and AdoMet concentrations. Solutions contained 0.1−1 μM enzyme in 50 mM Hepes·KOH and 50 mM KCl, pH 7.5, 25 °C. No activity was observed with 1 μM enzyme and 0.25 mM AdoMet in the presence of either 2 μM to 23 mM $Cr(aq)_6Cl_3$ or 0.1−500 mM NH_4Cl, KCl, or NaCl. $CuCl_2$, $ZnCl_2$, and $CdCl_2$ did not activate in the range of 1 μM to 1 mM. [b] In the presence of 20 mM EDTA.

With this background, the activation by a variety of ions was examined (Table 1 and Figure 1). Remarkably, some mono- and trivalent cations can activate *E. coli* AdoMetDC, while other ions of the same charges bind but do not activate. Table 1 lists the cation concentrations (K_a) for half-maximal activation and the associated Hill coefficients (n), the K_m values for AdoMet at the optimal cation concentration, and the V_{max} values. In no case was cooperativity observed for AdoMet saturation. For the lanthanides and Li^+ the enzymatic activity reached an optimum and then decreased with increasing concentration (not shown in Figure 1). For these ions the inhibition constant (K_i) was ~10-fold larger than the activator constant (K_a); the origin of the inhibition was not further investigated.

Monovalent Cations. Of the monovalent cation ions tested [Li^+, Na^+, K^+, Cs^+, NH_4^+, $(CH_3)_4N^+$] only Li^+ activated AdoMetDC, when concentrations as large as 0.5 M were tested for each. Higher Li^+ concentrations were required than other activating ions, all of which have greater charges (K_a = 331 mM; Figure 1). Activation was highly cooperative with a Hill coefficient of 4.0; this Hill coefficient is the same as the multiplicity of ($\alpha\beta$) units in the holoenzyme, indicating that binding of a single Li^+ ion may modify the behavior of the entire enzyme. Activation was less cooperative in the absence of KCl, with n = 1.8 and K_a = 83 mM. The maximal rate of AdoMet decarboxylation obtained with Li^+ was approximately the same as that observed with the presumed physiological activator, Mg^{2+}, and the K_m for AdoMet was ca. 2-fold higher.

Divalent Metal Ions. The ability of Ca^{2+}, Mn^{2+}, Fe^{2+}, Co^{2+}, Cd^{2+}, Ni^{2+}, and Zn^{2+} to activate AdoMetDC was tested under common reaction conditions (50 mM Hepes·KOH, pH

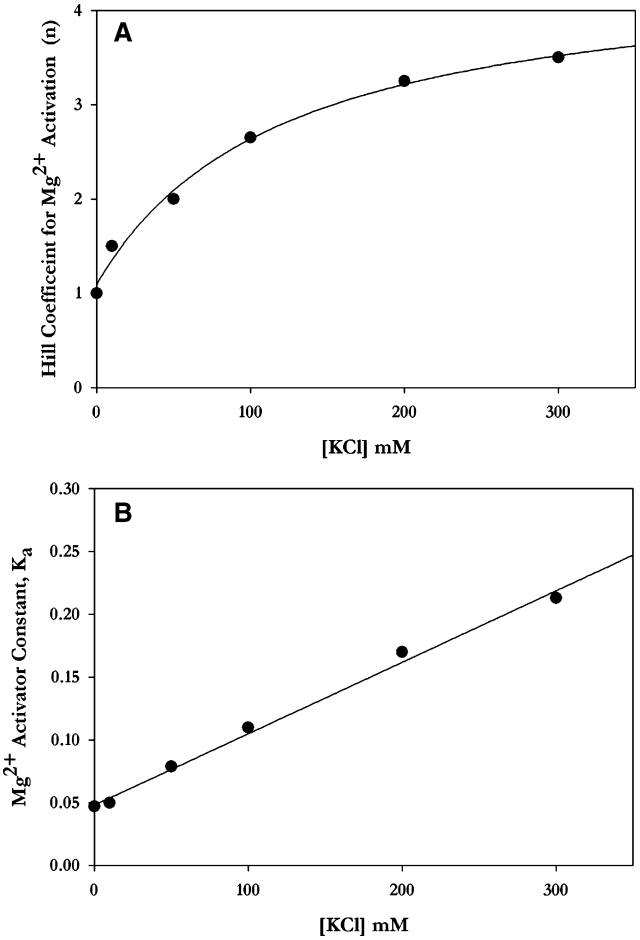

FIGURE 2: Variation in Hill coefficient for Mg^{2+} activation at different KCl concentrations. In Part A the line is a fit to a rectangular hyperbola with half-maximal change at 110 mM salt and a limiting Hill coefficient of 3.4. Part B shows the variation in activator constant (K_a) with KCl. The line is a linear fit with a slope of 0.0008. No activity (<0.1% of Mg^{2+}) was detected in the absence of Mg^{2+}. Solutions contained 1 mM AdoMet and 50 mM Hepes·KOH, pH 7.5 at 25 °C.

7.5, with 50 mM KCl) (Figure 1). Among the divalent metal ions, Fe^{2+} and Co^{2+} were found to be activators, as well as the known Ca^{2+} and Mn^{2+}, whereas Cu^{2+}, Zn^{2+}, and Ni^{2+} did not activate. The K_a values for Mn^{2+}, Co^{2+}, and Fe^{2+} are comparable to the K_a for Mg^{2+} (51, 38, and 90 μM vs 79 μM, respectively) while the V_{max} values are 45% of Mg^{2+} for Mn^{2+}, 29% for Co^{2+}, and 81% for Fe^{2+}. In each case the activation was positively cooperative with a Hill coefficient between 3 and 4 (Table 1). The K_m for AdoMet varied within an ~3-fold range from that with Mg^{2+}.

Trivalent Metal Ions. Three lanthanide ions (Tb^{3+}, Eu^{3+}, and Gd^{3+}) as well as Fe^{3+}, Al^{3+}, and the exchange-inert $Cr^{3+}(H_2O)_6$ and $Co^{3+}(NH_3)_6$ complexes were tested as potential activators. All three lanthanide ions activated, with K_a values of 1.5−3.8 μM, substantially lower than either Mg^{2+} or the divalent transition metal ion activators. Each of the lanthanides displayed cooperative activation with a Hill coefficient of ~4. When compared to Mg^{2+}, V_{max} values were 60% (Tb^{3+}), 45% (Gd^{3+}), and 72% (Eu^{3+}), and the K_m for AdoMet was within 2-fold of that with Mg^{2+}. Both Fe^{3+} and Al^{3+} cooperatively activated with V_{max} values 3.5% and 34% of Mg^{2+}, respectively. The K_m for AdoMet in the presence of Al^{3+} was 8.5-fold larger than the value with Mg^{2+}. The exchange-inert cation complex $Co^{3+}(NH_3)_6$ ion was also an activator; the K_a of 457 μM is 12 times higher than Co^{2+} (K_a = 38 μM); activation was insensitive to 20 mM EDTA, showing that it was not due to trace Co^{2+}. $Co(NH_3)_6^{3+}$ does not exchange first coordination sphere ligands on the time scale of <10 min used for the kinetic experiments (*29*); thus the Co^{3+} cannot become directly bound to the protein during the experiment. This result shows that activation can occur even if direct coordination of the cation to the substrate or protein is not possible. The failure of the exchange- inert $Cr^{3+}(H_2O)_6$ complex to activate is discussed below.

Table 2: Cation Binding Measured by Protein Fluorescence Changes[a]

cation	K_d, μM	n	ΔF (%)[b]
Li^+	(60 ± 5) × 10^3	1.7 ± 0.2	15 ± 1
Mg^{2+}	12 ± 2	0.9 ± 0.1	12 ± 1
Tb^{3+}	1.2 ± 0.2	1.4 ± 0.2	11 ± 1
Li^+	(131 ± 2) × 10^3 [c]	3.1 ± 0.2[c]	25 ± 1
Mg^{2+}	120 ± 2[c]	2.1 ± 0.1[c]	33 ± 1
Tb^{3+}	0.9 ± 0.1[c]	1.8 ± 0.1[c]	18 ± 1

[a] Solutions contained 10 mM Tris·HCl, pH 7.5, and 1 μM AdoMetDC. [b] ΔF is the percent change in fluorescence intensity. [c] Plus 50 mM KCl.

Fluorescence Studies of Cation Binding. Intrinsic protein fluorescence provides a sensitive spectroscopic probe of protein−ligand interactions and protein conformational transitions. Tryptophan and tyrosine residues serve as intrinsic fluorophores, the former being more sensitive because of a larger extinction coefficient and typically higher quantum yield (*30*). AdoMetDC from *E. coli* has only one tryptophan per ($\alpha\beta$) heterodimer (W249, which is 16 residues from the carboxy terminus); in addition, there are 14 tyrosine residues distributed throughout the sequence (*13*). Fluorescence studies were conducted in the absence of AdoMet. Initial experiments showed an excitation maximum of 280 nm and an emission maximum of 352 nm for the metal-free enzyme. Changes in fluorescence intensity accompanied metal ion binding for each cation examined, while the emission maximum remained 352 nm in the presence of the activating cations tested (Li^+, Mg^2, Tb^{3+}). The K_d values (half-maximal changes in fluorescence intensity) and the magnitude of the changes are listed in Table 2. Mg^{2+} binding became cooperative in the presence of KCl (or NaCl, KNO_3), as was observed when enzyme activation was monitored, and the K_d increased with salt concentration (see Figure 3). The half-maximal change in Hill coefficient occurred at 31 mM, and the maximal value was 3.8. Binding of Li^+, Mg^{2+}, and Tb^{3+} exhibited affinity and cooperativity reminiscent of their behavior in activity measurements; the emission intensity increased upon cation addition in each case. The presence of 50 mM KCl resulted in a decrease in the affinity of Li^+ and an increase in Hill coefficient, as was observed with Mg^{2+}. KCl did not substantially alter the binding of Tb^{3+}, which may be related to the higher affinity of Tb^{3+} and the need to use protein concentrations that approximate the dissociation constant for the activating cation. Saturable decreases in fluorescence were also observed upon addition of KCl and NaCl in the absence of activating cations, with half-maximal changes at 0.8 and 1.6 mM, respectively.

Studies of the Cation Effects on Protein Conformation. In view of the cooperative activation of the enzyme by cations, the possibility of a substantial alteration in protein conforma-

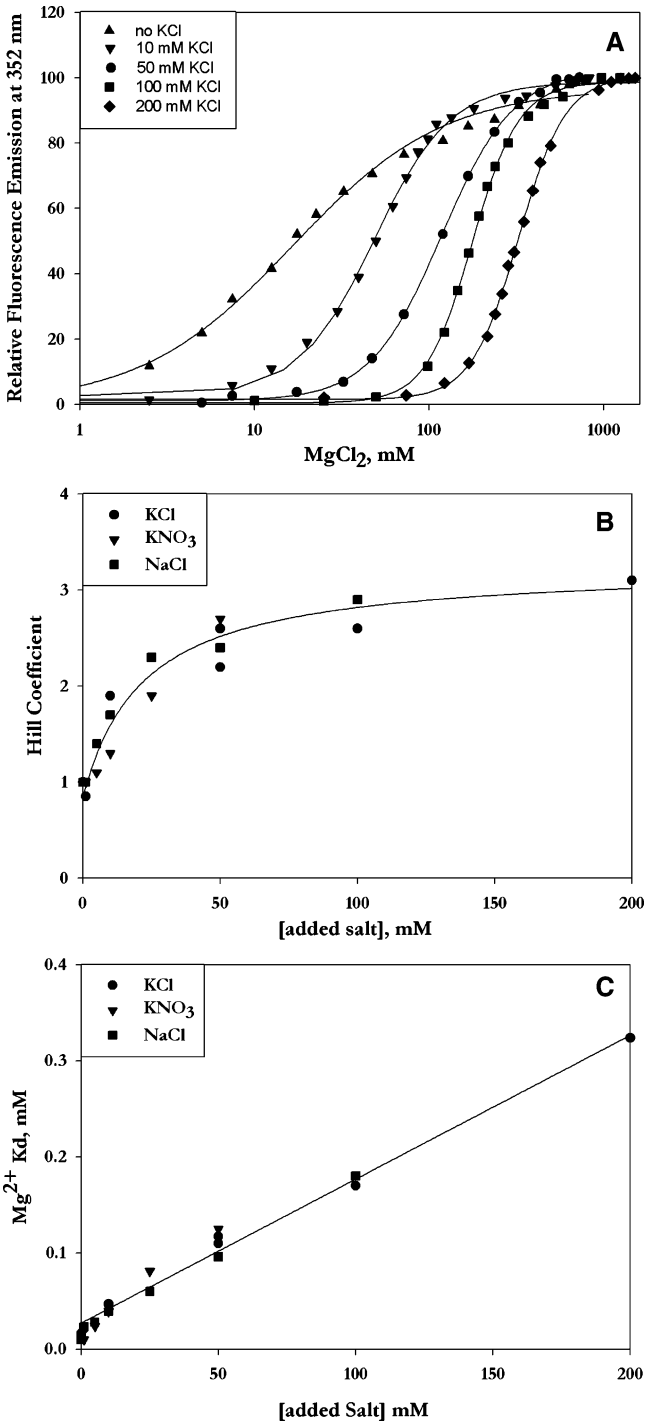

FIGURE 3: Changes in protein fluorescence upon addition of Mg^{2+}. Part A shows the fluorescence changes at 352 nm upon binding of Mg^{2+} in the presence of 0, 10, 50, 100, and 200 mM KCl. Lines are fits to the Hill equation with parameters illustrated in parts B and C. Part B shows the change in Hill coefficient for Mg^{2+} binding upon addition of KCl, NaCl, and KNO_3. The line is a fit of all the data to a rectangular hyperbola with half-maximal change at 26 mM salt and a limiting Hill coefficient of 3.3. Part C shows the variation in activator constant at different salt concentrations. The line is a linear fit to all of the data with a slope of 0.0014. Solutions contained 1 μM protein [($\alpha\beta$) subunits] in 10 mM Tris·HCl, pH 7.5 at 25 °C.

tion on binding was examined. CD was considered to be potentially informative because secondary structure prediction programs suggest a largely helical structure for the C-terminal protein segment containing the sole tryptophan. The protein CD spectrum was recorded in the 200−260 nm range in the absence of an activator and with either Mg^{2+} (10 mM), Tb^{3+}, (25 μM), or Gd^{3+} (25 μM) as representative ions. No spectral changes were observed, even in the presence of 50 mM KCl. Thus, there is no indication of a gross change in protein secondary structure in the presence of cation.

The possibility that the cations cause a change in the protein quaternary structure was assessed by dynamic light scattering measurements. The hydrodynamic radius of 49 Å changed by less than 5% upon addition of 50 mM KCl and/or 10 mM $MgCl_2$, showing that these ions neither alter the quaternary structure of the protein nor substantially modify the shape of the $(\alpha\beta)_4$ holoenzyme.

Inhibition by Zn^{2+}. Zn^{2+} was found to be a potent inhibitor of the enzyme. The activity of 1 μM enzyme was >99% inhibited by 25 μM Zn^{2+}, even when measured in the presence of 10 mM Mg^{2+} (Figure 4A). All of the activity was restored by incubation for 15 min with 5 mM EDTA, showing that inhibition is reversible. In contrast, activity was not restored by a 15 min incubation with 25 mM Mg^{2+} before activity was measured. Since Zn^{2+} has a propensity for binding to thiols, and AdoMetDCs have an essential active site cysteine as one of the few evolutionarily conserved residues (Cys-140 within *E. coli* AdoMetDC) (*31*), inhibition may be due to interaction with this cysteine (*19*, *21*). Uniquely among the ions tested, Zn^{2+} binding causes a blue shift in the maximum wavelength for protein fluorescence emission, from 352 to 342 nm (Figure 4B), indicating a conformational change involving movement of the tryptophan to a less polar environment (*32*). A dissociation constant of ~2 μM for Zn^{2+} was obtained by fluorescence titration. No change in the protein CD spectrum was observed in the presence of 10 μM $ZnCl_2$, indicating that the overall protein secondary structure was similar in the Zn^{2+} complex.

Dependence of Cation Interaction on pH. AdoMetDC activity varies significantly with pH, although the K_m for AdoMet does not change substantially (*17*). With either Mg^{2+} or Tb^{3+} as activator, in the presence or absence of 50 mM KCl, the pH profile for V_{max} was bell-shaped with pK values of 6.7 and 8.5 (Figure 5) with two protons involved on the acidic side. Thus, the charge of the cation does not substantially modulate the ionization of catalytically important residues.

DISCUSSION

The present results show that maximal activity of *E. coli* AdoMetDC alters little with metal ion charge; the K_m value for AdoMet and V_{max} values vary <30-fold in the presence of cations ranging in charge from +1 to +3 and even with the exchange-inert $Co(NH_3)_6^{3+}$ as activator. Previously, it was shown that the cation activator is required for trapping (and presumably formation) of a Schiff base complex with the product but not for noncovalent substrate/product binding to the enzyme (*17*). The ability of $NaCNBH_3$ to trap only the enzyme−product Schiff base complex suggests that a step in the reaction following decarboxylation is predominantly rate limiting in catalysis (*17*), and apparently this step is relatively insensitive to the nature of the activating cation. The solvent ^3H_2O kinetic isotope effect of 4.3 also supports a late rate-determining step (*33*). The common pH dependence of the Mg^{2+}- and Tb^{3+}-activated reactions shows that

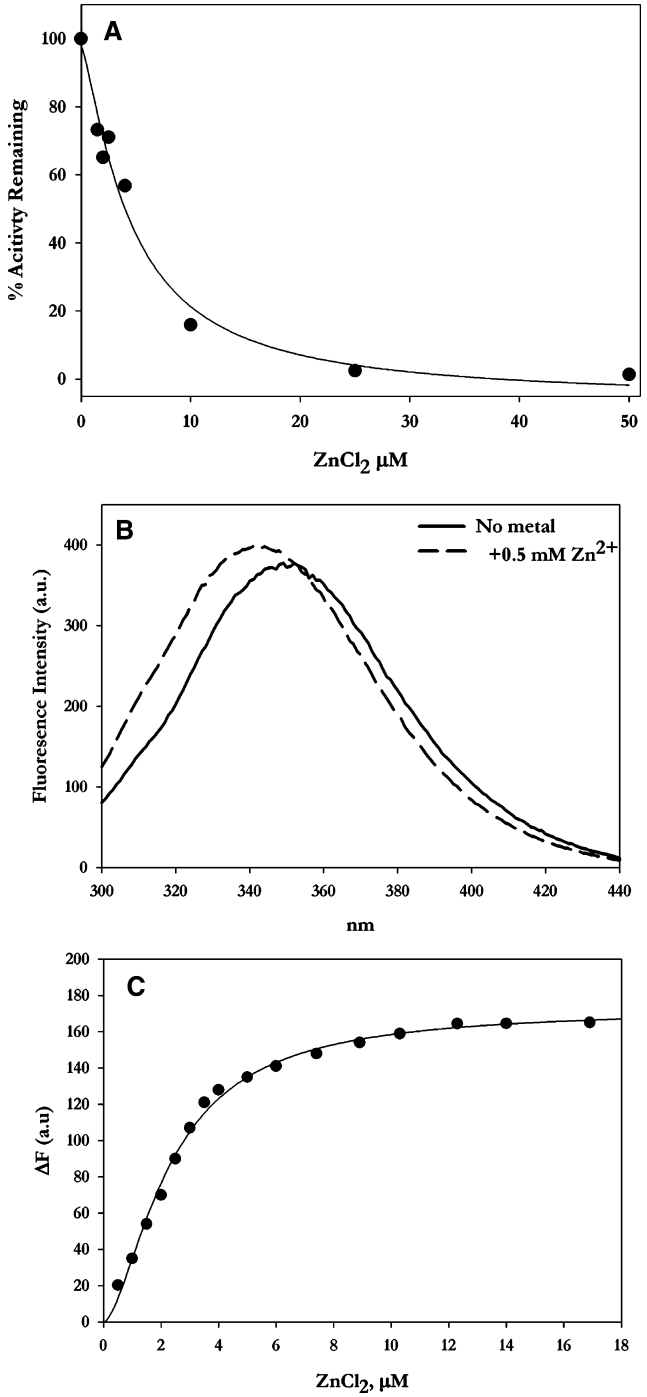

FIGURE 4: Inhibition of AdoMetDC by Zn^{2+}. Part A shows the reduction in enzyme activity upon addition of $ZnCl_2$ in the presence of 10 mM $MgCl_2$ and 0.2 mM AdoMet. The line is a fit to a rectangular hyperbola with half-maximal change at 4.5 μM $ZnCl_2$. Part B compares the fluorescence emission spectrum (with excitation at 280 nm) of 1 μM metal-free AdoMetDC with that observed in the presence of 0.5 mM $ZnCl_2$. Part C shows the change in fluorescence intensity at 342 nm upon addition of various concentrations of $ZnCl_2$. The line is a fit to the Hill equation with a K_d of 2.3 μM and $n = 1.6$. Solutions contained 10 mM Tris·HCl, pH 7.5 at 25 °C.

the ions do not modulate the ionization of catalytically essential residues. In conjunction with the cooperativity of cation activation, the results suggest an allosteric mechanism of cation activation.

The cation activation of *E. coli* AdoMetDC presents a surprisingly simple reflection of the properties of the ions.

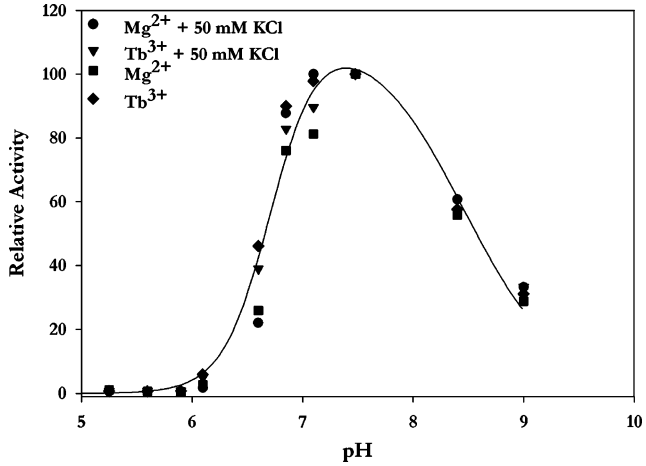

FIGURE 5: pH Dependence of V_{max} for the Mg^{2+} and Tb^{3+} activated enzyme in the presence and absence of 50 mM KCl. The symbols are as follows: (●) 10 mM $MgCl_2$, 50 mM KCl; (■) 10 mM $MgCl_2$; (▼) 10 μM $TbCl_3$, 50 mM KCl; (◆) 10 μM $TbCl_3$. Data are normalized to the rate observed at pH 7.5. The line is the fit of all data to a dependence on two protons with pK values of 6.7 on the acid side and one proton with a pK of 8.5 on the basic side.

The obvious initial discrimination is between hard and soft cations, which may in part reflect binding of soft ions in inhibitory modes, as is observed for Zn^{2+} which fluorescence measurements indicate causes protein structural distortions. The affinity of AdoMetDC for activating cations increases with formal charge, with an increment of ca. 10^2-10^3-fold per unit charge; a variation of a similar magnitude has been described for the Mg^{2+} site of the *E. coli* CheY signaling protein (*34*). The Mg^{2+} ion binding site of CheY consists of inner-sphere ligation by protein carboxylate groups; in this case the site is selective for cation charge rather than size, which was shown to be due to accommodation of various cation coordination numbers (*34*). However, the activation of AdoMetDC by the exchange-inert $Co(NH_3)_6^{3+}$ complex shows that inner-sphere ligation to protein residues is not absolutely required, although it may occur with other ions. It thus appears that the AdoMetDC activators can bind as aquo complexes through an outer-sphere interaction with the protein.

The dissociation constants for the ions, determined by protein fluorescence changes, are similar to the activator constants. When the ΔG for binding $[-RT \ln(1/K_a)]$ is plotted versus the charge to radius ratio of the activating ions, a linear relationship is seen for most ions, with the notable exceptions of Al^{3+}, Fe^{3+}, and $Co(NH_3)_6^{3+}$ (Figure 6 and Table 3). For the data in the linear range the slope is -372 ± 56 (kcal/mol)/(e^-/pm), showing an electrostatic dependence of the affinity. The deviations of Fe^{3+}, $A1^{3+}$, and Co^{3+}-$(NH_3)_6$ from the linear relationship are readily understood. The aquo ferric ion has a pK near 2.2, thus under our conditions it is present as $Fe(H_2O)_5(OH)^{2+}$, effectively a divalent hydrate (*35*). The aquo Al^{3+} has a complex speciation at neutral pH [pK_a values of 5.5, 5.8, 6.0, and 6.3 for the $Al(H_2O)_6^{3+}$ through $Al(H_2O)_3(OH)_3$ series, as well as oligomer formation (*36*)]; thus which component activates is not readily discerned. $Co(NH_3)_6^{3+}$ can only form outer-sphere complexes; therefore, the effective ionic radius is much larger than that of the Co^{3+} ion alone.

The selectivity of AdoMetDC is not solely based on ionic radius, which is in contrast to the typical behavior of enzymes

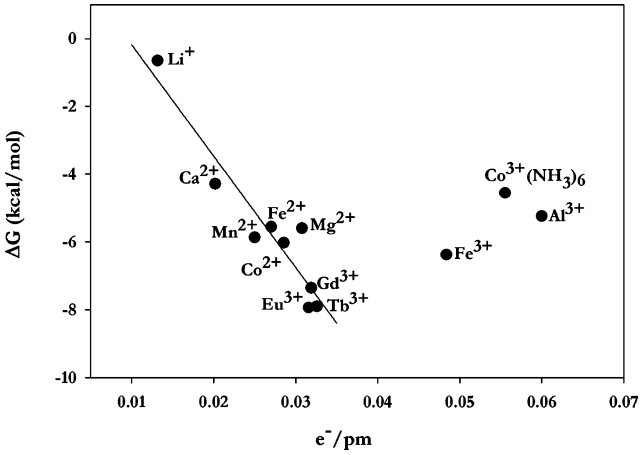

FIGURE 6: Variation in ΔG for metal ion activation with the charge/radius ratio of the cations. The line is a linear fit to the data excluding Fe^{3+}, Al^{3+}, and $Co^{3+}(NH_3)_6$, as described in the text. The slope of the line is −372 (kcal/mol)/(e^-/pm).

Table 3: Metal Ion Radii and Activation of AdoMet Decarboxylase[a]

ion	K_a, mM	radius, pm coord no. = 6 (*52*)	charge/radius, e^-/nm
Li^{+} [b]	331	76	13.1
Mg^{2+}	0.079	65	30.7
Ca^{2+}	0.73	99	20.2
Mn^{2+}	0.051	80	25.0
Fe^{2+}	0.090	74	27.0
Co^{2+}	0.038	70	28.6
Fe^{3+}	0.13	62	48.4
Co^{3+} [b,c]	0.46	54	55.5
Al^{3+}	0.14	50	60.0
Tb^{3+}	0.0016	92	32.6
Eu^{3+}	0.0015	95	31.5
Gd^{3+}	0.0038	94	31.9
Na^{+} [e]	1.6	95	10.5
K^{+} [e]	3.0	133	7.5
Cs^{+}		169	5.9
NH_4^{+}			
Cu^{2+}		69[d]	28.9
Cd^{2+}		91	21.9
Zn^{2+} [e]	0.001	71[d]	28.2
Ni^{2+}		66	30.3
Cr^{3+} [b]		58	34.5

[a] In 50 mM Hepes·KOH and 50 mM KCl, pH 7.5. No activity was observed with 1 μM enzyme and 0.25 mM AdoMet in the presence of either 2 μM to 23 mM $Cr(aq)_6Cl_3$ or 0.1−500 mM NH_4Cl, KCl, or NaCl. $CuCl_2$, $ZnCl_2$, and $CdCl_2$ did not activate in the range of 1 μM to 1 mM. [b] In the presence of 20 mM EDTA. [c] As $Co^{3+}(NH_3)_6$. [d] For 4-coordination. [e] From fluorescence titration.

that are specific for ions of a certain charge, among which ionic radius is often a secondary criterion in selectivity; dialkylglycine decarboxylase is exemplary of this behavior (*37*). In dialkylglycine decarboxylase the cation size causes a switch between active complexes with K^+ or Rb^+ and inactive complexes with Na^+ or Li^+ (*37*); two protein ligands present in the active complexes are replaced by a single water molecule in the inactive complexes, resulting in enlargement of the protein structure in the vicinity of the ion. In dialkylglycine decarboxylase both cation size and charge are determining factors in ion affinity, activation, and substrate affinity (*38*). In contrast, the Ca^{2+} binding sites of EF-hand proteins have strong selectivity based on ion size rather than charge, thus accepting trivalent lanthanide ions while discriminating against the smaller Mg^{2+} (*39*).

The tolerance of AdoMetDC for ions differing in preferred coordination number is remarkable. Activators vary in ligation number preference from 4 for the small Li^+ ion, to the strong preference of Mg^{2+} for six ligands (*40*), to the malleable lanthanides for which the coordination number readily varies from 6 to 8 (*39*, *41*). This is in stark contrast to many Mg^{2+}-activated enzymes in which octahedral coordination is nearly mandatory (*1*, *42*).

Also remarkable is that activation does not require either exchangeable ligands or even the presence of a first coordination sphere water molecule, in contrast to most divalent cation activated enzymes (*42*). Thus the activation by $Co(NH_3)_6^{3+}$ shows that the binding does not require displacement of inner-sphere ligands, and inner-sphere water molecules from the cation complex are clearly not involved in the decarboxylase reaction. There have been other reports of enzyme activation by exchange-inert metal ion complexes of Cr^{3+} or Co^{3+}, with aquo or amino ligands (*29*, *42*−*44*). The coordination exchange- inert $Cr(H_2O)_6^{3+}$ complex, but not the $Co(NH_3)_6^{3+}$ ion, activates enzymes such as the *E. coli* exonuclease III, suggesting the importance of inner-sphere water molecule(s) (*29*, *45*). In contrast, $Co(NH_3)_6^{3+}$ activates ribonuclease H, showing that an outer-sphere interaction suffices (*43*). The robust activation of AdoMetDC by $Co(NH_3)_6^{3+}$ contrasts with the failure of aquo Cr^{3+} to activate. This difference may reflect the ionization properties of the metal complexes. The first pK_a of $Cr(H_2O)_6^{3+}$ is ca. 4, yielding $Cr(H_2O)_5(OH)^{2+}$, while a second pK_a near 7 yields $Cr(H_2O)_4(OH)_2^{+}$, which will be a significant portion of the total Cr^{3+} species under our conditions (*29*). Thus a distinction between the Cr^{3+} and Co^{3+} complexes used (following the obvious substitution of water by the more weakly hydrogen-bonding and less easily ionized NH_3) is that under our reaction conditions the net charge on the cobalt complex will be 3+ while the chromium complexes will have a reduced net charge, and a vastly reduced effective charge/radius ratio, when compared to Mg^{2+}, for example.

Among monovalent cation activated enzymes the primary selectivity is defined by cation charge, but then a secondary selectivity in terms of ionic radius is typically observed (*2*, *3*, *46*). A few examples of Li^+ binding to Mg^{2+} sites are known. High affinity of an inhibitory Li^+ has been found for the Mg^{2+} binding site of phosphoglucomutase (*47*). The crystal structures of the Mg^{2+}-activated enzymes 3′-phosphoadenosine-5′-phosphatase and *myo*-inositol monophosphatase, both of which are inhibited by lithium, have been interpreted as having a 4-coordinate Li^+ replacing one of the three octahedrally coordinated Mg^{2+} ions. We are not aware of another enzyme for which a monovalent cation activates in place of Mg^{2+} (*48*, *49*).

The AdoMetDC fluorescence emission maximum of 352 nm approaches that of free tryptophan and indicates that this residue is largely solvent exposed (*32*). It is thus noteworthy that cation binding largely changes the emission intensity without substantial changes in the wavelength of the emission maximum. Only the inhibitory Zn^{2+} causes a change in the environment of the fluorophore. In the absence of structural data conclusions regarding the physical basis for the spectroscopic phenomena are as yet unwarranted.

Attempts at redesigning the cation specificity of proteins have been described (*50*). While alteration of binding

selectivity toward cations of differing charge has been achieved (*34*), the elimination of a cation requirement for maximal protein function typically has not been obtained, with the notable exception of pyruvate kinase where a single amino acid change abolished the monovalent cation requirement (*51*). AdoMetDC presents a case where nature has found a simple and tolerant solution to metal ion utilization. The structural basis for binding and activation will rely upon ongoing studies.

ACKNOWLEDGMENT

We thank Drs. H. and C. W. Tabor for the plasmid used to overproduce AdoMet decarboxylase. We thank Drs. E. K. Jaffe, L. Tang, and M. A. Pimkin for helpful discussions. We thank Dr. Lei Tang for performing the light scattering experiments. We appreciate the advice of Dr. H. Roder on the fluorescence experiments. We thank Drs. J. Peterson and Y. Matsumoto, who graciously made their fluorometers available to us. The Spectroscopy Support Facility, the Computing and Information Technology Facilities, and the Biochemistry and Biotechnology Facilities contributed to this work.

REFERENCES

1. Glusker, J. P. (1991) Structural aspects of metal liganding to functional groups in proteins, *Adv. Protein Chem. 42*, 1−76.
2. Di Cera, E. (2006) A structural perspective on enzymes activated by monovalent cations, *J. Biol. Chem. 281*, 1305−1308.
3. Suelter, C. H. (1970) Enzymes activated by monovalent cations, *Science 168*, 789−795.
4. Page, M. J., and Di Cera, E. (2006) Role of Na^+ and K^+ in enzyme function, *Physiol. Rev. 86*, 1049−1092.
5. Dudev, T., and Lim, C. (2003) Principles governing Mg, Ca, and Zn binding and selectivity in proteins, *Chem. Rev. 103*, 773−788.
6. Tabor, C. W., and Tabor, H. (1984) Polyamines, *Annu. Rev. Biochem. 53*, 749−790.
7. Fontecave, M., Atta, M., and Mulliez, E. (2004) *S*-Adenosylmethionine: nothing goes to waste, *Trends Biochem. Sci. 29*, 243−249.
8. Markham, G. D., Norrby, P. O., and Bock, C. W. (2002) *S*-Adenosylmethionine conformations in solution and in protein complexes: conformational influences of the sulfonium group, *Biochemistry 41*, 7636−7646.
9. Kim, A. D., Graham, D. E., Seeholzer, S. H., and Markham, G. D. (2000) *S*-Adenosylmethionine decarboxylase from the archaeon *Methanococcus jannaschii*: identification of a novel family of pyruvoyl enzymes, *J. Bacteriol. 182*, 6667−6672.
10. Sekowska, A., Coppee, J. Y., Le Caer, J. P., Martin-Verstraete, I., and Danchin, A. (2000) *S*-Adenosylmethionine decarboxylase of *Bacillus subtilis* is closely related to archaebacterial counterparts, *Mol. Microbiol. 36*, 1135−1147.
11. Tabor, C. W., and Tabor, H. (1984) Methionine adenosyltransferase (*S*-adenosylmethionine synthetase) and *S*-adenosylmethionine decarboxylase, *Adv. Enzymol. Relat. Areas Mol. Biol. 56*, 251−282.
12. Hackert, M. L., and Pegg, A. E. (1997) Pyruvoyl-Dependent enzymes, *Comp. Biochem. Catal. 2*, 201−216.
13. Tabor, C. W., and Tabor, H. (1987) The speEspeD operon of *Escherichia coli*. Formation and processing of a proenzyme form of *S*-adenosylmethionine decarboxylase, *J. Biol. Chem. 262*, 16037−16040.
14. van Poelje, P. D., and Snell, E. E. (1990) Pyruvoyl-dependent enzymes, *Annu. Rev. Biochem. 59*, 29−59.
15. Pegg, A. E., Xiong, H., Feith, D. J., and Shantz, L. M. (1998) *S*-Adenosylmethionine decarboxylase: structure, function and regulation by polyamines, *Biochem. Soc. Trans. 26*, 580−586.
16. Toney, M. D. (2001) Computational studies on nonenzymatic and enzymatic pyridoxal phosphate catalyzed decarboxylations of 2-aminoisobutyrate, *Biochemistry 40*, 1378−1384.
17. Markham, G. D., Tabor, C. W., and Tabor, H. (1982) *S*-Adenosylmethionine decarboxylase of *Escherichia coli*. Studies on the covalently linked pyruvate required for activity, *J. Biol. Chem. 257*, 12063−12068.
18. Wickner, R. B., Tabor, C. W., and Tabor, H. (1970) Purification of adenosylmethionine decarboxylase from *Escherichia coli* W: evidence for covalently bound pyruvate, *J. Biol. Chem. 245*, 2132−2139.
19. Ekstrom, J. L., Mathews, I., Stanley, B. A., Pegg, A. E., and Ealick, S. E. (1999) The crystal structure of human *S*-adenosylmethionine decarboxylase at 2.25 Å resolution reveals a novel fold, *Struct. Folding Des. 7*, 583−595.
20. Bennett, E. M., Ekstrom, J. L., Pegg, A. E., and Ealick, S. E. (2002) Monomeric *S*-adenosylmethionine decarboxylase from plants provides an alternative to putrescine stimulation, *Biochemistry 41*, 14509−14517.
21. Toms, A. V., Kinsland, C., McCloskey, D. E., Pegg, A. E., and Ealick, S. E. (2004) Evolutionary links as revealed by the structure of *Thermotoga maritima S*-adenosylmethionine decarboxylase, *J. Biol. Chem. 279*, 33837−33846.
22. Kashiwagi, K., Taneja, S. K., Xie, Q. W., Tabor, C. W., and Tabor, H. (1988) *S*-adenosylmethionine decarboxylase from *Escherichia coli* and from *Saccharomyces cerevisiae*: cloning and overexpression of the genes, *Adv. Exp. Med. Biol. 250*, 73−79.
23. Mehta, P. K., and Christen, P. (2000) The molecular evolution of pyridoxal-5′-phosphate-dependent enzymes, *Adv. Enzymol. 74*, 129−183.
24. Pegg, A. E. (1974) Purification of rat liver *S*-adenosyl-L-methionine decarboxylase, *Biochem. J. 141*, 581−583.
25. Li, Y. F., Hess, S., Pannell, L. K., White Tabor, C., and Tabor, H. (2001) *In vivo* mechanism-based inactivation of *S*-adenosylmethionine decarboxylases from *Escherichia coli*, *Salmonella typhimurium*, and *Saccharomyces cerevisiae*, *Proc. Natl. Acad. Sci. U.S.A. 98*, 10578−10583.
26. Anton, D. L., and Kutny, R. (1987) *Escherichia coli S*-adenosylmethionine decarboxylase. Subunit structure, reductive amination, and NH_2-terminal sequences, *J. Biol. Chem. 262*, 2817−2822.
27. Mach, H., Middaugh, C. R., and Lewis, R. V. (1992) Statistical determination of the average values of the extinction coefficients of tryptophan and tyrosine in native proteins, *Anal. Biochem. 200*, 74−80.
28. Lu, Z. J., and Markham, G. D. (2004) Catalytic properties of the archaeal *S*-adenosylmethionine decarboxylase from *Methanococcus jannaschii*, *J. Biol. Chem. 279*, 265−273.
29. Black, C. B., and Cowan, J. A. (1997) Inert chromium and cobalt complexes as probes of magnesium-dependent enzymes. Evaluation of the mechanistic role of the essential metal cofactor in *Escherichia coli* exonuclease III, *Eur. J. Biochem. 243*, 684−689.
30. Ross, J. B. A., Laws, W. R., W., R. K., and Wyssbord, H. R. (1992) Tyrosine fluorescence and phosphorescence from proteins and polypeptides, in *Topics in Fluorescence Spectroscopy*, pp 1−63, Plenum Press, New York.
31. Diaz, E., and Anton, D. L. (1991) Alkylation of an active-site cysteinyl residue during substrate-dependent inactivation of *Escherichia coli S*-adenosylmethionine decarboxylase, *Biochemistry 30*, 4078−4081.
32. Reshetnyak, Y. K., Koshevnik, Y., and Burstein, E. A. (2001) Decomposition of protein tryptophan fluorescence spectra into log-normal components. III. Correlation between fluorescence and microenvironment parameters of individual tryptophan residues, *Biophys. J. 81*, 1735−1758.
33. Allen, R. R., and Klinman, J. P. (1981) Stereochemistry and kinetic isotope effects in the decarboxylation of *S*-adenosylmethionine catalyzed by the pyruvyl enzyme, *S*-adenosylmethionine decarboxylase, *J. Biol. Chem. 256*, 3233−3239.
34. Needham, J. V., Chen, T. Y., and Falke, J. J. (1993) Novel ion specificity of a carboxylate cluster Mg(II) binding site: strong charge selectivity and weak size selectivity, *Biochemistry 32*, 3363−3367.
35. Huheey, J. E., Keiter, E. A., and Keiter, R. L. (1997) *Inorganic Chemistry, Principles of Structure and Reactivity*, Benjamin Cummings, Reading, MA.
36. Swaddle, T. W., Rosenqvist, J., Yu, P., Bylaska, E., Phillips, B. L., and Casey, W. H. (2005) Kinetic evidence for five-coordination in $AlOH(aq)^{2+}$ ion, *Science 308*, 1450−1453.

37. Hohenester, E., Keller, J. W., and Jansonius, J. N. (1994) An alkali metal ion size-dependent switch in the active site structure of dialkylglycine decarboxylase, *Biochemistry 33*, 13561−13570.
38. Liu, W., and Toney, M. D. (2004) Kinetic and thermodynamic analysis of the interaction of cations with dialkylglycine decarboxylase, *Biochemistry 43*, 4998−5010.
39. Pidcock, E., and Moore, G. R. (2001) Structural characteristics of protein binding sites for calcium and lanthanide ions, *J. Biol. Inorg. Chem. 6*, 479−489.
40. Markham, G. D., Glusker, J. P., and Bock, C. W. (2002) The arrangement of first- and second-sphere water molecules in divalent magnesium complexes: Results from molecular orbital and density functional theory and from structural crystallography, *J. Phys. Chem. B 106*, 5118−5134.
41. Dudev, T., Chang, L. Y., and Lim, C. (2005) Factors governing the substitution of La^{3+} for Ca^{2+} and Mg^{2+} in metalloproteins: a DFT/CDM study, *J. Am. Chem. Soc. 127*, 4091−4103.
42. Cowan, J. A. (2002) Structural and catalytic chemistry of magnesium-dependent enzymes, *Biometals 15*, 225−235.
43. Jou, R., and Cowan, J. A. (1991) Ribonuclease H activation by inert transition-metal complexes. Mechanistic probes for metallocofactors: Insights on the metallobiochemistry of divalent magnesium ion, *J. Am. Chem. Soc. 113*, 6685−6686.
44. Maguire, M. E., and Cowan, J. A. (2002) Magnesium chemistry and biochemistry, *Biometals 15*, 203−210.
45. Suga, H., Cowan, J. A., and Szostak, J. W. (1998) Unusual metal ion catalysis in an acyl-transferase ribozyme, *Biochemistry 37*, 10118−10125.
46. Markham, G. D. (2003) Monovalent cation activation of IMP dehydrogenase, in *Inosine Monophosphate Dehydrogenase: A Major Therapeutic Target*, pp 169−183, American Chemical Society, Washington, DC.
47. Ma, C., and Ray, W. J., Jr. (1980) Structural comparisons among the central complexes in the phosphoglucomutase system by means of spectral techniques, *Biochemistry 19*, 751−759.
48. Gill, R., Mohammed, F., Badyal, R., Coates, L., Erskine, P., Thompson, D., Cooper, J., Gore, M., and Wood, S. (2005) High-resolution structure of myo-inositol monophosphatase, the putative target of lithium therapy, *Acta Crystallogr., Sect. D: Biol. Crystallogr. 61*, 545−555.
49. Albert, A., Yenush, L., Gil-Mascarell, M. R., Rodriguez, P. L., Patel, S., Martinez-Ripoll, M., Blundell, T. L., and Serrano, R. (2000) X-ray structure of yeast Hal2p, a major target of lithium and sodium toxicity, and identification of framework interactions determining cation sensitivity, *J. Mol. Biol. 295*, 927−938.
50. Prasad, S., Wright, K. J., Banerjee, R. D., Bush, L. A., Cantwell, A. M., and Di Cera, E. (2003) Redesigning the monovalent cation specificity of an enzyme, *Proc. Natl. Acad. Sci. U.S.A. 100*, 13785−13790.
51. Laughlin, L. T., and Reed, G. H. (1997) The monovalent cation requirement of rabbit muscle pyruvate kinase is eliminated by substitution of lysine for glutamate 117, *Arch. Biochem. Biophys. 348*, 262−267.
52. Brown, I. D. (1988) What factors determine cation coordination numbers, *Acta Crystallogr. B44*, 545−553.

BI6025962